Regular Article

PHYSICAL CHEMISTRY RESEARCH
Published by the
Iranian Chemical Society
www.physchemres.org
info@physchemres.org

Phys. Chem. Res., Vol. 12, No. 1, 145-156, March 2024
DOI: 10.22036/pcr.2023.374464.2248

Coupling Interaction of Ampicillin Drug with Ninhydrin in Aqueous Acidic Medium: Kinetics and Mechanistic Studies

T.A. Ibrahim[a], E.S.H. Khaled[b], R.A. Mohamed[b], M.M. Abdel-Hafeez[a] and A.A. Abdel-Khalek[b,*]

[a]*Expert in Forensic Medicine Authority, Cairo-Egypt*

[b]*Chemistry Department, Faculty of Science, Beni-Suef University, Beni-Suef City, Egypt*

(Received 28 November 2022, Accepted 1 June 2023)

The kinetics of Ninhydrin (Nin) reaction with Ampicillin (Amp) has been studied in an aqueous acidic medium. The product of the reaction was examined spectroscopically using Nuclear magnetic resonance (^{1}H NMR) and Infrared spectra in addition to Ultra-performance liquid chromatography (UPLC). The reaction was monitored spectrophotometrically, with (0.1-0.4) × 10^{-4} mol dm^{-3} of Amp, (0.5-5.0) × 10^{-2} mol dm^{-3} Nin and 0.3-0.9 mol dm^{-3} ionic strength (I) over the (30-50) °C range of temperature. It is first order with respect to [Nin] and [Amp], decreases as pH increases in the range (4.70-6.04). The thermodynamics activation parameters involving ΔH^* and ΔS^* have been calculated. The rate of the reaction follows the rate law d[Amp-Nin]/dt ={(k3+k2[H+])[Nin]}×[Amp]. For this reaction is proposed mechanism was supported by an excellent isokinetic relationship between ΔH^* and ΔS^* for some Nin reactions. In emergency cases, poisoning with Amp, about 30% of the oral dose is excreted in urine as unchanged drug within 6 h, so in clinical toxicology, a presumptive colour test is necessary. Consequently, the use of Nin to form a coupling coloured complex with Amp is an effective method.

Keywords: Kinetics, Reaction mechanism, Ninhydrin, Ampicillin

INTRODUCTION

Because of its sensitivity in the analysis of the amino group, Nin is widely used in a variety of fields, including the quantitative determination of amino acids containing both an amino group and a carboxylic group compound, particularly amino acids with an amino group bonded directly to the carbon [1]. Furthermore, it is used in bioanalytical studies, particularly in the field of forensic medicine, to visualize developed fingerprints [2]. Another important role of Nin is in its use for residual protein detection on re-usable surgical instruments, where the instrument surfaces are swabbed with rayon swabs wetted with water and dipped in Nin and heated for up to one hour at about 60 °C [3,4]. If the swab turns purple, this means the instrument must be rewashed due to protein contamination.

*Corresponding author. E-mail: king_elsafey@yahoo.com

Proteins are polymers of amino acids and are linked through peptide bonds. So, the estimation of peptides is much more vital to evaluating protein structure. The quantitative reaction of the Nin reagent with the -amino N-terminal groups of peptides is used to determine peptides [5,6]. Also, the reaction of Nin with the metal-peptide complex was studied. In addition to the latest uses, Nin has been extensively used for the analysis and characterization of compounds in microbiological, biomedical, histochemical, food, clinical, plant, and nutritional studies [7]. It is widely used in determining pharmaceutical compounds in addition to kinetic studies [8,9].

Ampicillin is a broad-spectrum antibiotic used to treat bacterial diseases since 1961 [10] and it belongs to the aminopenicillin family, which is mainly used to treat many bacterial infections such as respiratory infections, urinary tract infections, meningitis, salmonellosis, and endocarditis (from the heart) [11-13].

Ampicillin is part of the penicillin group of beta-lactams and is a member of the aminopenicillin family [14,15].

Ampicillin can penetrate gram-positive bacteria as well as several gram-negative bacteria. It is only different from penicillin or benzylpenicillin because of the presence of amino groups [16]. This amino group present in ampicillin helps it pass through the hole of the Gram-negative bacterial external membrane. Ampicillin acts as an irreversible inhibitor of the enzyme transpeptidase, and this ultimately leads to cytolysis by preventing the third and final step of bacterial cell wall synthesis in the double division [17,18].

The mechanism of reactions is passing through the attack on the carbonyl-carbon of Nin by the lone pair of electrons of nitrogen in the amino acid, yielding a Schiff base. The Schiff base undergoes hydrolysis rapidly and produces 2-aminoindanedione, which is very reactive and reacts with another molecule of Nin to yield a purple-colored product (called Ruhemann's purple) [1].

The current study investigates the possibility of formation Amp-Nin coupling. Our work is studying factors that affect the rate of its formation, suggesting a suitable mechanism, and proving its validity. This coupling interaction is an effective method that can be used in emergency cases to identify poisoning with Amp.

MATERIALS AND METHODS

Chemicals and Solutions

All analytical chemicals (Aldrich, Merck, and Sigma) were used as supplied without further purification. CH_3COONa/CH_3COOH buffer of known concentration was used. The ionic strength was adjusted by means of $NaNO_3$ in the solution. Freshly prepared solutions of Nin were used. Doubly distilled H_2O was used in all kinetic runs.

Instrumentation

The reaction rate was measured by monitoring the absorption of the product on the Jenway 6300 spectrophotometer, equipped with a temperature cell support and connected to a thermal circulating water bath. A double-beam spectrophotometer, JASCO UV-630, was used to measure the UV-Vis absorption spectra of the reaction product of Amp with Nin.

The pH measurements of all the reaction mixtures were performed using a Chertsey, Surrey, 7065 pH meter.

Product formation was confirmed by a chromatography method using the Dionex Series of High-Performance Liquid Chromatography (UPLC) 3000. It is supplied with a quaternary pump, Autosampler, different column sets, a mobile phase with a flow rate range from 0.1 to 10 ml min^{-1}, and a DAD detector which can scan samples from 190 to 900 nm (UV and visible region).

Also, the Amp-Nin complex as a product was examined with the ^1H NMR technique, using BRUKER AVANCE III, 400 MHz equipped with triple resonance helium-cooled cryoprobe, broadband probe, 3.2 and 4 mm solids probes, and 4 mm HRMAS probe, automatic sample changer, and variable temperature capability.

The Fourier transform infrared (FT-IR) spectrum was recorded on a Vertex 70 FT-IR instrument (Bruker Company). The sample was carefully mixed with KBr as a matrix that was grounded and pressed with a special press to yield a standard-diameter disk. The disc formed was examined in the 4000 to 400 cm^{-1} range.

Kinetics Procedures

Experiments were run by using a large excess (10-fold) of Nin over Amp in all runs to maintain pseudo-first-order conditions. The ionic strength was kept constant by the addition of the appropriate volume of $NaNO_3$ solution and the pH of the reaction mixture was found constant during the reaction runs. The reaction was initiated by mixing the reagents from the previously thermostated solutions, with the exception of Nin, with the required quantity of separate thermostated stock solution from Nin.

RESULTS AND DISCUSSION

Stoichiometry

The number of moles of Amp consumed with respect to Nin to form the coupling was performed using an excess of Amp (10 folds) than Nin and the absorbance of the product was measured after 24 h from the begging of the reaction at λ_{max} 565 nm. The concentration ratio was found to be 2 moles of Nin for one mole of Amp as illustrated in Table 1.

Table 1. Stoichiometric Results for Reaction of Amp with Nin

10^3 [Amp] (mol dm^{-3})	10^4 [Nin] (mol dm^{-3})	10^4 [product] (mol dm^{-3})	[Nin]/ [product]
1	1	0.649	1.54
2	2	1.11	1.80
3	3	1.60	1.87

Therefore, the stoichiometry of the reaction can be represented by Eq. (1):

$$\text{Amp} + 2\text{Nin} \rightarrow \text{product} \quad (1)$$

Product Analysis

UV-Vis absorption of the product. The spectrum of the product of Amp with Nin was recorded between 350 and 750 nm with time, during the reaction, a purple color appeared which absorbed maximally at 565 nm and its intensity was increased gradually with time from the initiation of time up to one hour as shown in Fig. 1.

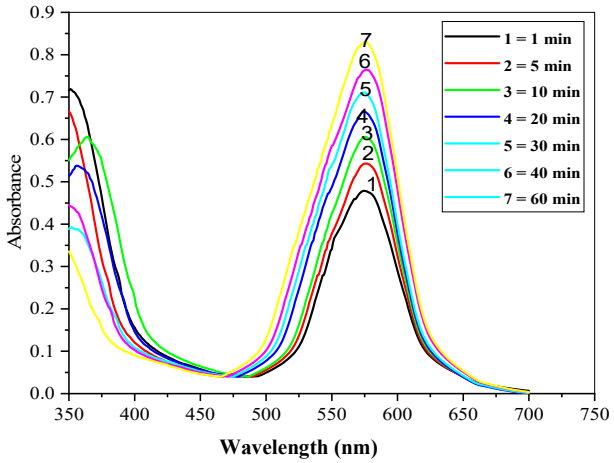

Fig. 1. Change of absorbance as a function of time at 1, 5, 10, 20, 30, 40, and 60 min, respectively at pH = 5.07, Amp = 1 × 10^{-4} mol dm^{-3}, [Nin] = 2.5 × 10^{-2} mol dm^{-3}, I = 0.20 mol dm^{-3} and T = 30 °C.

Ultra-performance liquid chromatography. It is a unique method that was used to ensure the formation of the Amp-Nin coupling. The chromatographic separation was performed on a C_{18} column with a 65:35 (v/v) mixture of

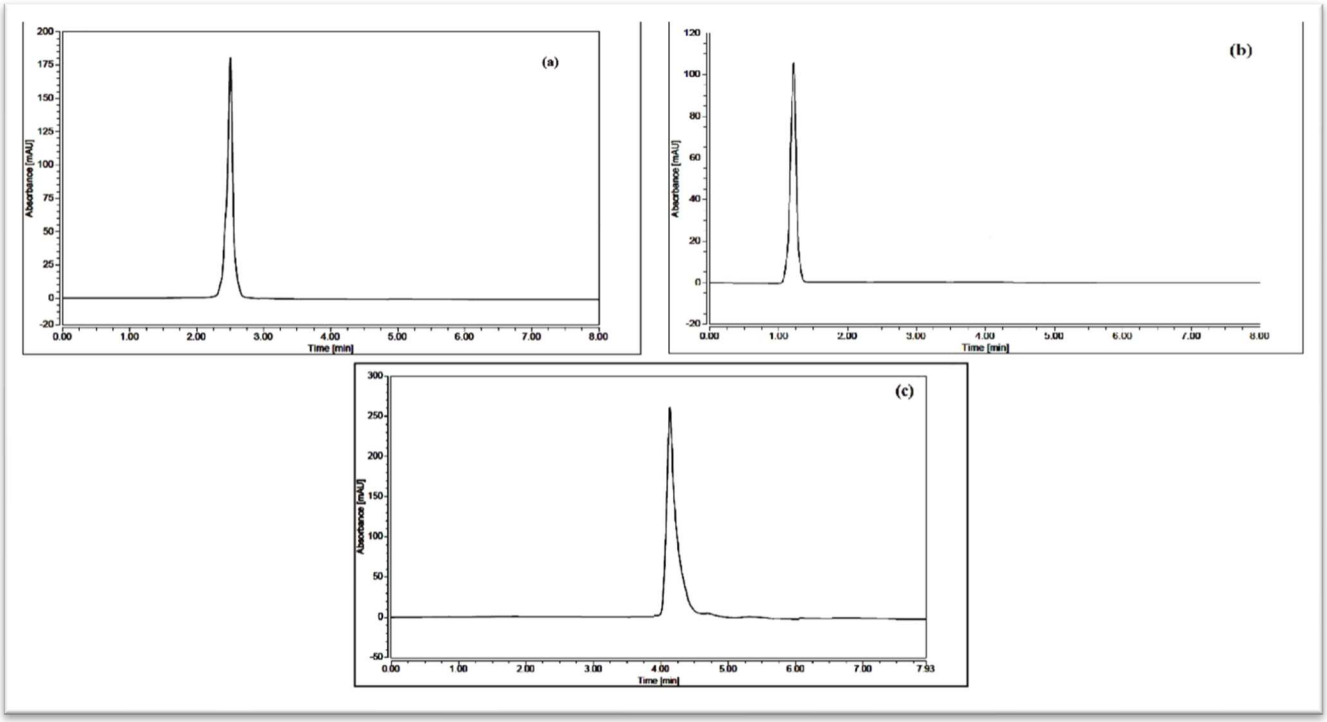

Fig. 2. UPLC of Amp-Nin coupling (a), Amp (b), and Nin (c).

10 mM phosphate buffer, pH was 3.6, and acetonitrile as the mobile phase. The UPLC spectrum of 2.5×10^{-4} mol dm^{-3} of; Amp-Nin coupling, Amp, and Nin appeared at maximum peak at a retention time of 2.34 min, 1.26 min, and 4.28 min, respectively (Figs. 2a, b, c). The difference in the retention time of the appearance of the absorption bands identifies the formation of the Amp-Nin complex [19].

Spectroscopic studies. Nuclear magnetic resonance spectra: Figure 3A shows the ^{1}H NMR spectrum of Amp-Nin coupling, the peak at 12.80 ppm was assigned to the OH proton of alcohol, and the broad multiple peaks appearing between 9.45 and 10.60 ppm showed eight aromatic CH protons of two benzene rings. In the spectra of the coupling compound, it is apparent that an effect is exerted on the NH_2 protons, which are completely diminished [20-23]. Figure 3B shows ^{13}C NMR spectra (100 MHz, DMSO, δ, ppm): 119.80, C(5,8), 121.90, C(1), 124.50, C(3), 124.80, C(4), 130.30, C(2), 157 132.10, C(6,7), 133.3, C(12), 137.20, C(9,10), 142.7, C(18), 143.50, C(11), 160.30, C(16,17), 197.70, 177.40, C(13), 180.90, C(14), C(15) [24-26].

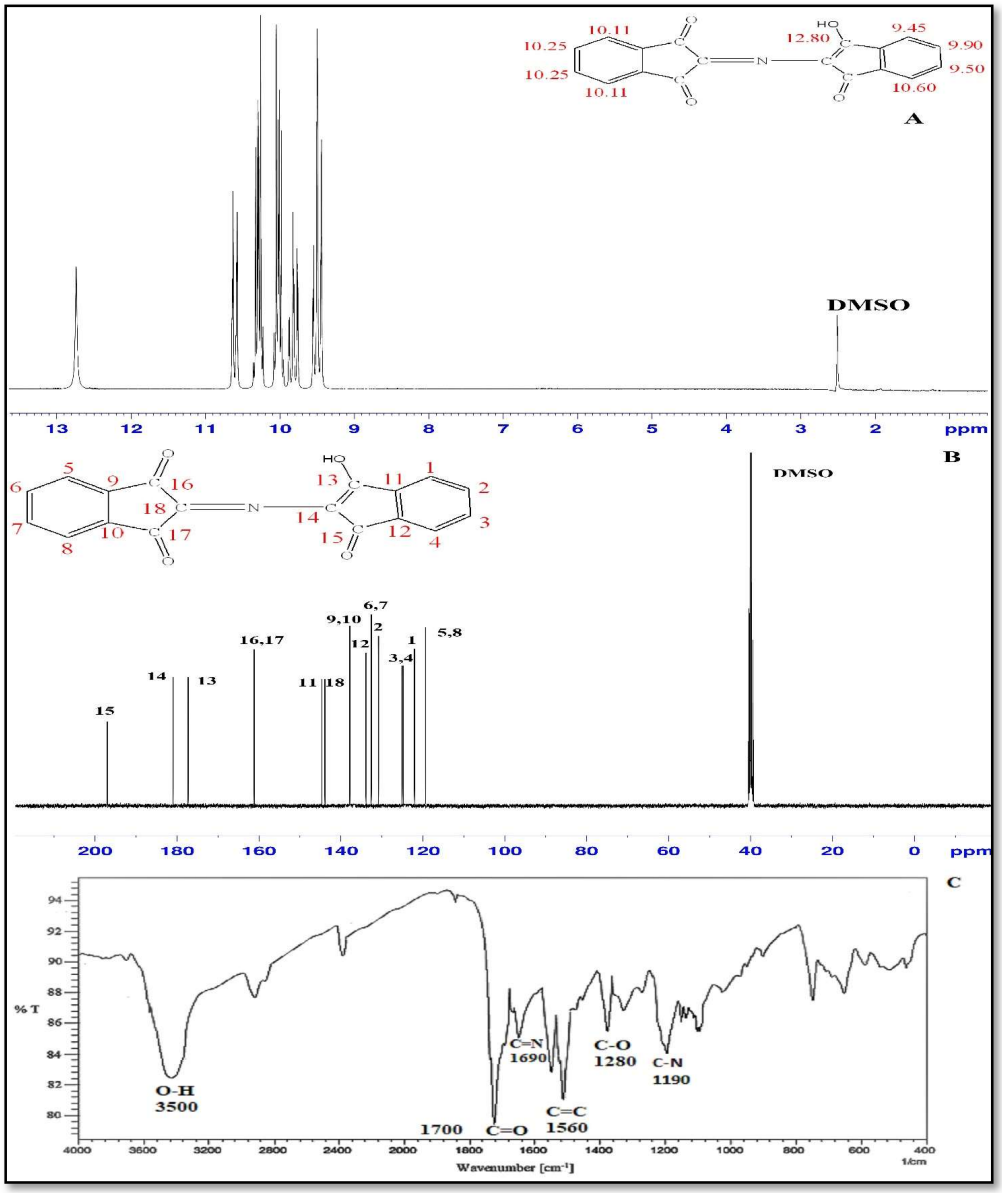

Fig. 3. Spectroscopic analysis for Amp-Nin coupling; ^{1}H NMR spectra (A), ^{13}C NMR spectra (B), and FTIR spectra (C).

Infrared spectra: The FT-IR spectra of the Amp-Nin coupling were represented graphically in Fig. 3C. From which, the two sharp broad bands at 3300 and 3250 cm^{-1} owing to O–H stretching of Nin completely diminished in the complex spectra and showed the main absorption bands of its structural-functional groups O-H stretching vibration broadband around 3500 cm^{-1}, 1700 cm^{-1} stretching vibration C=O, 1690 cm^{-1} stretching vibration C=N, 1280 cm^{-1} stretching vibration C-O, 1190 cm^{-1} stretching vibration C-N, C=C group absorption at 1560 cm^{-1} remained in its position [27].

Kinetics of Amp/Nin Reaction

The conditions of the pseudo-first-order were applied to this reaction where the concentration of Nin was kept in excess than that of Amp with more than ten-fold at least where the used ranges of Amp and Nin were (0.1-0.4) × 10^{-4} and (0.5-5.0) × 10^{-2} mol dm^{-3}, respectively. Plots of ln (A_∞-A_t) with time were linear for about 85% from the beginning of the reaction where A_∞ and A_t are the absorbance at time infinity and time t, respectively. Using version 9.5 of the Microcal Origin program, the error limits for results were calculated.

Rate dependence on Amp concentration. Using different concentrations of Amp of (1, 3, 5, 7, 9) × 10^{-4} mol dm^{-3}, pH = 5.07, [Nin] = 2.5 × 10^{-2} mol dm^{-3}, I = 0.10 mol dm^{-3} and T = 30 °C, the observed pseudo-first-order rate constant (k_{obs}) values were (14.43, 14.87, 15.28, 14.91, 14.79) × 10^{-3}, respectively. These values indicate the independence of k_{obs} on the concentration of Amp and the order with respect to Amp is first order.

Also, the first-order kinetics was confirmed from plots of log[Amp-Nin]/dt *vs*. log[Amp] where the relation was linear with a slope equal nearly to unity, then:

$$d[Amp\text{-}Nin]/dt = k_{obs}[Amp]_T \quad (2)$$

Rate dependence on Nin concentration. The dependence of k_{obs} on the concentration of Nin was determined by carrying out the kinetic experiments at pH = 5.07, [Amp] = 1.0 × 10^{-4} mol dm^{-3}, I = 0.10 mol dm^{-3} over a range of Nin concentration of (0.5-5.0) × 10^{-2} mol dm^{-3} and different temperatures from 30 °C up to 50 °C (Table 2) P lots of k_{obs} *vs*. [Nin] were linear without intercepts, as shown in Fig. 4, and can be described as:

$$k_{obs} = k_1 [Nin] \quad (3)$$

Where k_1 is constant.

Effect of pH on the rate of the reaction. It is a very important factor that was investigated due to effecting of the product formation by the pH of the reaction medium. Over the (4.70-6.04) range of pH and the other parameters were

Table 2. Variation of k_{obs} with [Nin] at [Amp] = 1.0 × 10^{-4} mol dm^{-3}, pH = 5.07, I = 0.10 mol dm^{-3} and Different Temperatures

10^2 [Nin] (mol dm^{-3})	10^3 k_{obs} min^{-1} ± SD				
	T = 30 °C	T = 35 °C	T = 40 °C	T = 45 °C	T = 50 °C
0.5	3.14 ± 0.124	3.75 ± 0.217	3.88 ± 0.151	4.10 ± 0.126	4.19 ± 0.181
1.0	5.43 ± 0.123	7.35 ± 0.083	9.05 ± 0.076	10.79 ± 0.127	12.51 ± 0.152
1.5	8.64 ± 0.122	10.18 ± 0.124	13.76 ± 0.107	16.25 ± 0.113	19.03 ± 0.144
2.0	12.49 ± 0.202	14.55 ± 0.176	18.23 ± 0.081	20.66 ± 0.134	24.67 ± 0.153
2.5	14.43 ± 0.123	17.95 ± 0.202	21.86 ± 0.113	25.78 ± 0.161	30.13 ± 0.122
3.0	16.28 ± 0.071	21.15 ± 0.124	25.73 ± 0.088	29.90 ± 0.155	36.87 ± 0.164
3.5	18.84 ± 0.092	24.76 ± 0.156	29.61 ± 0.126	33.72 ± 0.173	42.58 ± 0.145
4.0	21.13 ± 0.164	27.65 ± 0.054	32.64 ± 0.114	37.34 ± 0.186	47.53 ± 0.126
4.5	23.07 ± 0.115	29.58 ± 0.123	35.76 ± 0.103	42.53 ± 0.192	52.52 ± 0.157
5.0	26.33 ± 0.125	32.03 ± 0.087	39.64 ± 0.201	48.20 ± 0.171	57.71 ± 0.143

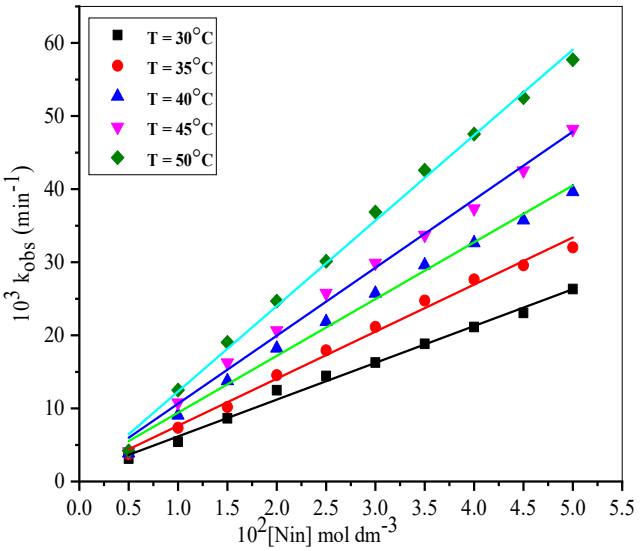

Fig. 4. dependence of k_{obs} on the concentration of Nin.

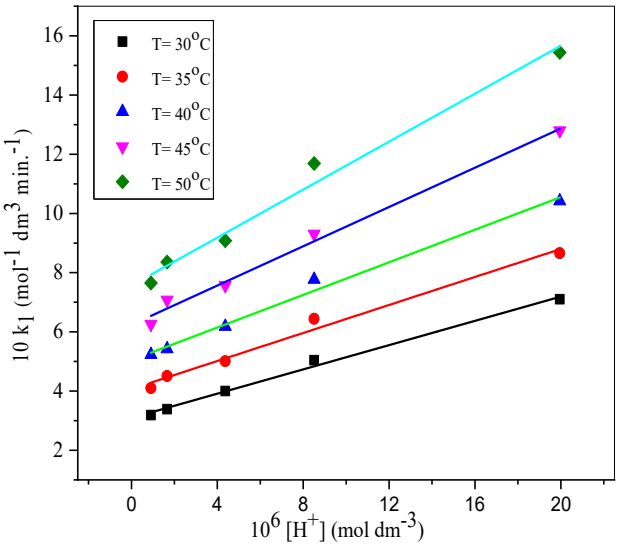

Fig. 5. Variation of k_1 with H^+ at different temperatures.

kept constant, the effects of the pH were studied. The obtained kinetics data are represented in Table 3 from which the reaction rates decreased as pH increased over the range studied. Plots of k_1 with [H^+] at different temperatures were linear with different slopes, k_2, and intercepts, k_3 as shown in Fig. 5.

This effect can be described by Eq. (4) as follow;

$$k_1 = k_3 + k_2 [H^+] \quad (4)$$

Equation (4) indicates that there are two pathways for the reaction. The first one is dependent on [H^+] with a rate constant k_2 and k_3 is the rate constant of the second independent pathway.

Effect of temperature on the rate of the reaction and thermodynamic activation parameters. The effect of temperature on the interaction of Amp with Nin was carried out at 30, 35, 40, 45, and 50 °C whereas the other conditions were [Amp] = 1.0×10^{-4} mol dm^{-3}, I = 0.10 mol dm^{-3} over ranges of [Nin] and pH of $(0.5\text{-}5.0) \times 10^{-2}$ mol dm^{-3} and (4.70-6.04), respectively. As shown in Fig. 4, the rate of the reaction increased as the temperature increased. From Fig. 5, values of k_2 and k_3 were determined at different temperatures and collected in Table 4.

Activation parameters are believed to provide useful information regarding the environment in which chemical reactions take place. Using Eyring Equation,

Table 3. Variation of k_1 with [H^+] at Different Temperatures

pH	10^6[H^+] (mol dm^{-3})	$10k_1$ (mol^{-1} dm^3 min^{-1}) ± SD				
		T = 30 °C	T = 35 °C	T = 40 °C	T = 45 °C	T = 50 °C
4.70	19.95	7.10 ± 0.11	8.66 ± 0.16	10.42 ± 0.18	12.80 ± 0.22	15.44 ± 0.27
5.07	8.51	5.04 ± 0.15	6.44 ± 0.19	7.77 ± 0.14	9.31 ± 0.17	11.69 ± 0.40
5.36	4.37	4.00 ± 0.11	5.01 ± 0.10	6.18 ± 0.07	7.57 ± 0.11	9.08 ± 0.13
5.78	1.66	3.39 ± 0.08	4.51 ± 0.09	5.42 ± 0.07	7.08 ± 0.15	8.36 ± 0.11
6.04	0.91	3.19 ± 0.06	4.10 ± 0.08	5.23 ± 0.09	6.26 ± 0.06	7.65 ± 0.06

Table 4. Variation of k_2 and k_3 with Temperature

T (°C)	$k_3 \times 10$ (mol^{-2} dm^6 min^{-1}) ± SD	$k_2 \times 10^7$ (mol^{-2} dm^6 min^{-1}) ± SD
30	3.09 ± 0.19	20.49 ± 0.019
35	4.07 ± 0.16	23.65 ± 0.216
40	5.04 ± 0.65	27.53 ± 0.119
45	6.24 ± 0.48	33.16 ± 0.315
50	7.56 ± 0.23	40.50 ± 0.215

$$\ln k/T = (\ln ƙ/h + \Delta S^*/R) - \Delta H^*/RT \quad (5)$$

(Where ƙ is the Boltzmann constant, h is Planck's constant, R is the universal gas constant and T is the absolute temperature).

Values of ΔH^* and ΔS^* are calculated from the slope and intercept of the plot of ln(k/T) against 1/T, respectively. ΔH^* and ΔS^* for the two pathways dependent and independent on $[H^+]$ are calculated from plots of $\ln(k_2/T)$ and $\ln(k_3/T)$ against 1/T, respectively as shown in Fig. 6 and Fig. 7. The enthalpies of activation, ΔH^*_2, and ΔH^*_3 were calculated as 28.81 ± 0.13 and 37.99 ± 0.05 kJ mol^{-1}, respectively. The corresponding entropies of activation, ΔS^*_2, and ΔS^*_3 are -266.97 ± 0.14 and -137.68 ± 0.06 J K^{-1} mol^{-1} respectively. The positive value of ΔH* obtained indicates that the reaction is endothermic, and the smallest value of the enthalpy of activation indicates the formation of the more solvated complex. Factors controlling ΔH* are closely related to those controlling ΔS*, and their contributions to the rate constant appear to compensate for each other. As a result, the composite negative value of ΔS* is mostly negative, which can be explained by the ordering of the solvated water molecules in the equilibrium reactions and final product.

Effect of ionic strength on the rate of the reaction. The rate of the reaction was unaffected by ionic strength, where the k_{obs} values were (14.43 ± 0.005, 14.62 ± 0.001, 15.07 ± 0 .001, 13.76 ± 0.007, 14.72 ± 0.005, 15.21 ± 0.001 and 14.86 ± 0 .001) × 10^{-3} min^{-1} at I = 0.3, 0.4, 0.5, 0.6, 0.7, 0.8 and 0.9 mol dm^{-3} when the other factors kept constant at; pH = 5.07, [Nin] = 2.5 × 10^{-2} mol dm^{-3} and T = 30 °C. The independence of reaction rate on ionic strength demonstrates that the reaction involves, at least, one of the reactant species being uncharged. In our case, the uncharged species is Nin.

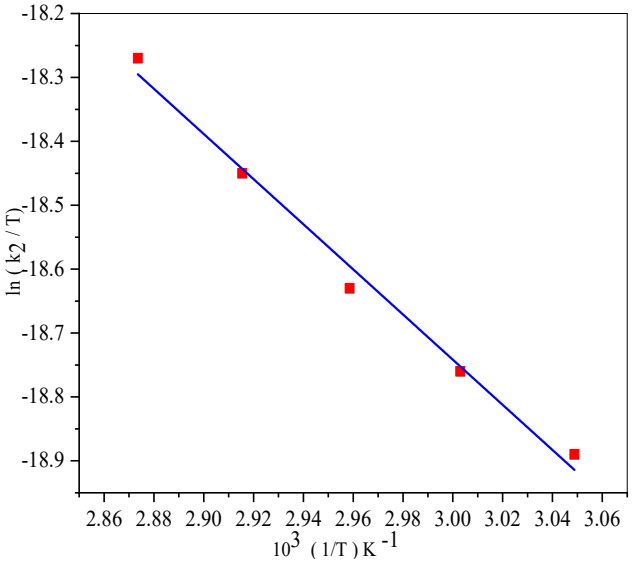

Fig. 6. Variation of $\ln k_2/T$ against 1/T.

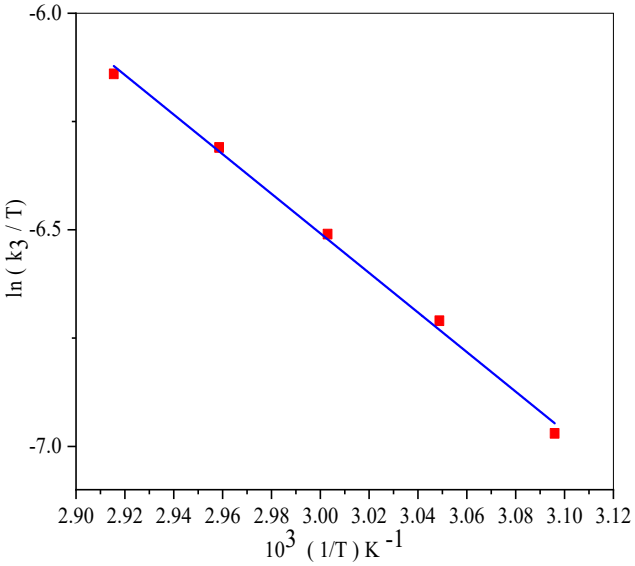

Fig. 7. Variation of $\ln k_3/T$ against 1/T.

From Eqs. (2)-(4), the experimental rate law for coupling interaction is formulated in Eq. (6):

$$d[Amp\text{-}Nin]/d\,t = \{(k_3 + k_2[H^+])[Nin]\}[Amp] \quad (6)$$

Where,

$$k_{obs} = (k_3 + k_2([H^+])[Nin]\} \quad (7)$$

Discussion

The experimental rate law of the reaction of Amp with Nin in an aqueous acidic medium appears dependent on $[H^+]$ suggesting the involvement of the protonated form of Nin beside the unprotonated one in the rate-determining step. Then, the following equilibrium can be expected;

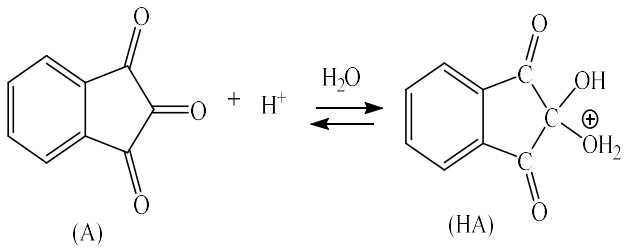

Where the A form has been considered as the reactive species of the AH one. Amp contains a primary aliphatic amino group so, in the reaction of Nin (A) with Amp (B) a nucleophilic attack of the free lone pair of electrons of nitrogen of the amino group of Amp will attack the partially positive charge present on the carbon of the carbonyl group to produce Schiff base. In pH lower than 5.0, the Schiff base isn't stable and hydrolyzed very fast to form an intermediate (C) according to the Scheme 1. Where (C) is a very reactive intermediate that reacts with the second molecule of Nin to yield a purple-coloured product and Scheme 2 can be expected. During the reaction, the protonated species of Nin (AH) will participate in the reaction by reacting with Amp to form an intermediate (D) which reacts with the second molecule of Nin to give a product according to the Scheme 3.

In the light of the above discussions and the experimental results, the following mechanism for the reaction may be proposed:

$$(A) + (H^+) \rightleftharpoons (AH) \quad K_6 \quad (8)$$

$$(A) + (B) \rightleftharpoons (A\text{---}B) \quad K_7 \quad (9)$$

$$(AH) + (B) \rightleftharpoons (AH\text{---}B) \quad K_8 \quad (10)$$

$$(A\text{---}B) \xrightarrow{r.d.s.} product \quad k_9 \quad (11)$$

$$(AH\text{---}B) \xrightarrow{r.d.s.} product \quad k_{10} \quad (12)$$

The rate of the reaction from the above mechanism can be described by the following equation;

$$Rate = k_9[A\text{---}B] + k_{10}[AH\text{---}B] \quad (13)$$

Using steady state for [A---B]:

$$K_7[A][B] = K_{-7}[A\text{---}B] + k_9[A\text{---}B \quad (14)$$

Then;

$$[A\text{---}B] = K_7[A][B]/(K_{-7} + k_9) \quad (15)$$

Using steady state for [AH---B]

$$K_8[AH][B] = K_{-8}[AH\text{---}B] + k_{10}[AH\text{---}B] \quad (16)$$

Then;

$$[AH\text{---}B] = K_8[AH][B]/(K_{-8} + k_{10}) \quad (17)$$

From Eq. (8),

$$[AH] = K_6[A][H^+] \quad (18)$$

From Eqs. (17) and (18);

$$[AH\text{---}B] = K_6 K_8[A][H^+][B]/(K_{-8} + k_{10}) \quad (19)$$

By substitution from Eqs. (15) and (19) in Eq. (13) one gets;

$$Rate = \{k_9 K_7[A][B]/(K_{-7} + k_9)\} + \{(k_{10} K_6 K_8[A][H^+][B]/(K_{-8} + k_{10})\} \quad (20)$$

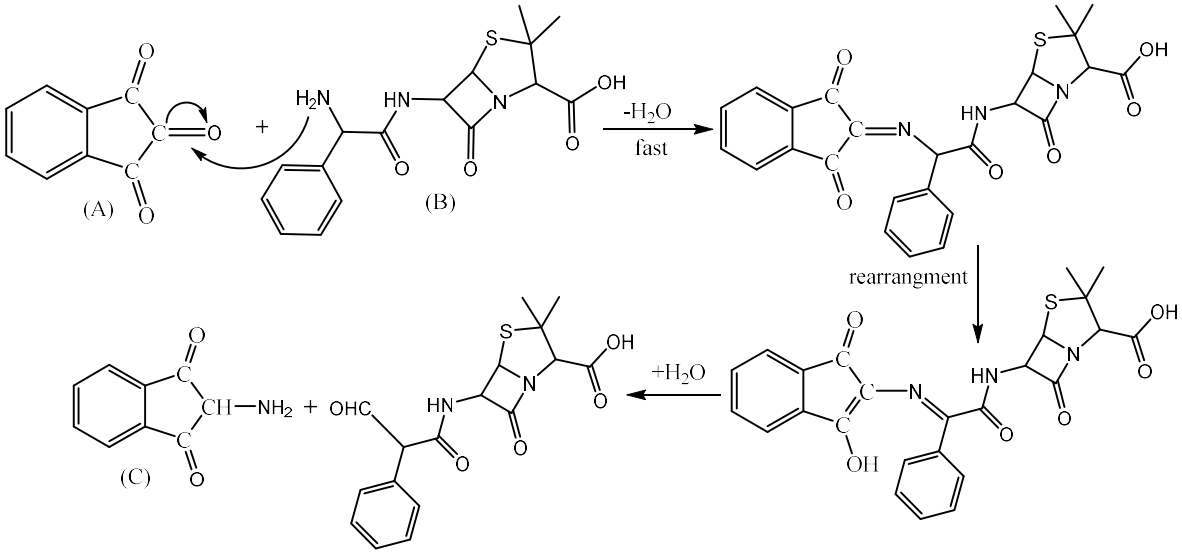

Scheme 1. Formation of the intermediate C

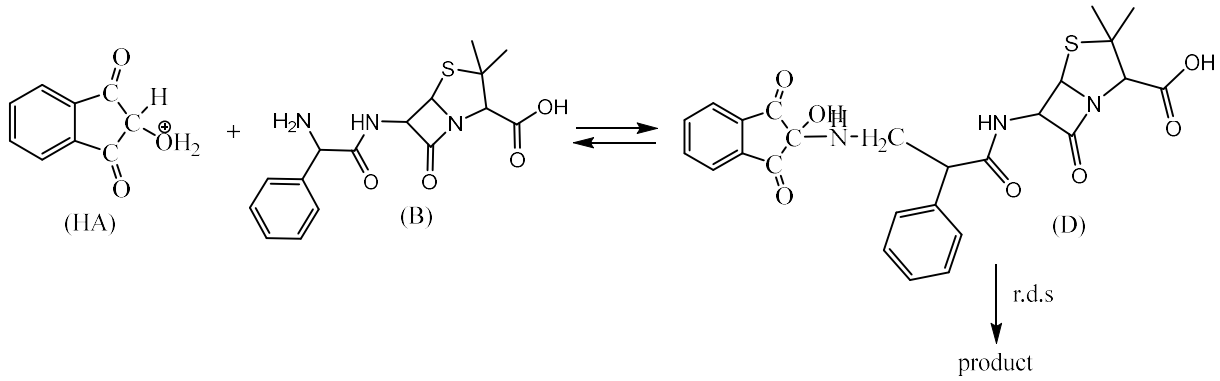

Scheme 2. Formation of the product

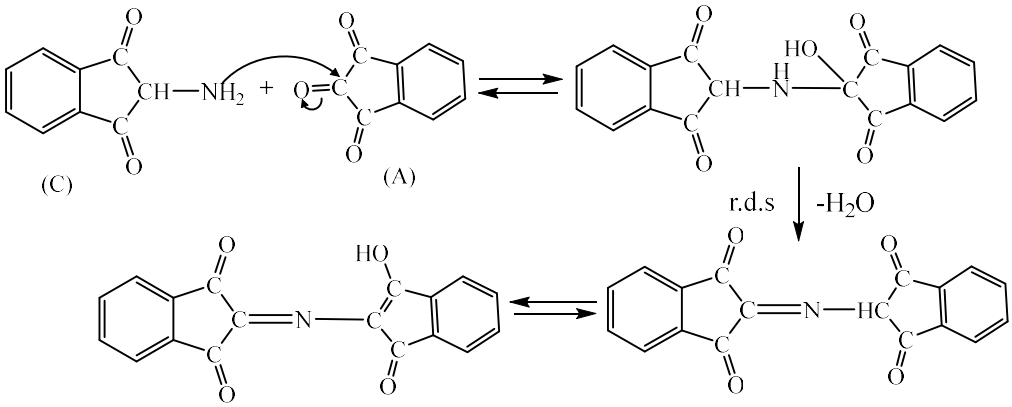

Scheme 3. Reaction of AH with B

On rearrangement, the following equation can be obtained;

$$\text{Rate} = [A][B]\{(k_9 K_7/(K_{-7} + k_9)) + (k_{10} K_6 K_8/(K_{-8} + k_{10}))[H^+]\} \quad (21)$$

Where

$$k_{obs} = \{(k_9 K_7/(K_{-7} + k_9)) + (k_{10} K_6 K_8/(K_{-8} + k_{10}))[H^+]\}[B] \quad (22)$$

From Eqs. (7) and (22) the derived k_{obs} is identical to the experimental rate law then;

$$k_2 = (k_{10} K_6 K_8/(K_{-8} + k_{10}) \quad (23)$$

and

$$k_3 = \{(k_9 K_7/(K_{-7} + k_9)\} \quad (24)$$

ΔH^* is a composite value including the enthalpy of formation associated with the formation of AH---B and the enthalpy of activation of the product. The obtained positive value of ΔH^* means that the reaction is endothermic and the smallest value of the enthalpy of activation gives an indication of the formation of a more solvated complex. Factors that control ΔH^* are closely related to those controlling ΔS^* where their contributions to the rate constant seem to compensate for each other. Therefore, the composite negative value of ΔS^* is largely and this can be interpreted as a result of the ordering of the solvated water molecules of the equilibrium reactions and final product. The last suggested mechanism for the Nin-Amp reaction can be supported by plotting the relationship between ΔH* and ΔS* of other reactions for Nin (Table 5) as shown in Fig. 8. There is a parallel change in ΔH* and ΔS* values of these reactions that reflects a common mechanism for such closely related reactions.

Table 5. Values of ΔH* and ΔS* for some Reactions of Nin

Substances	ΔS^* (J K^{-1} mol^{-1})	ΔH^* (kJ mol^{-1})	Ref.
Phenylalanine	-10(0.6	79.6	[28]
Valine	-88.0 5	73.7	[28]
Methionine	-184	49.3	[29]
Amp	-266.97	28.81	This work

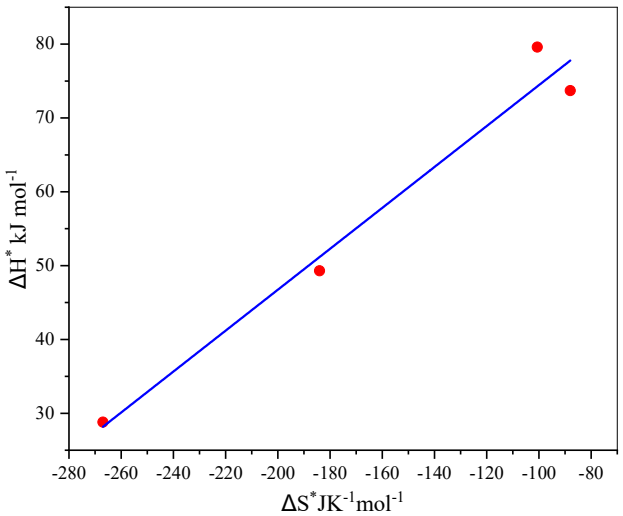

Fig. 8. Isokinetic relationship for some reactions of Nin.

CONCLUSION

The product of coupling of Nin with Amp was examined and the reaction was studied kinetically; it was first-order with respect to [Amp] and [Nin]. The rate was decreased as pH increased over the range studied while increased as the temperature increased revealing the endothermic nature of the reaction. A suggested mechanism in which the protonated and unprotonated species of Amp are involved in the reaction with Nin where the protonated one is considered as the reactive species. This mechanism was promoted with an isokinetic relationship for some reactions of Nin. This coupling is necessary as presumptive test in clinical toxicology.

REFERENCES

[1] Kumar, D.; Rub, M. A., Role of cetyltrimethylammonium bromide (CTAB) surfactant micelles on kinetics of [Zn (II)-Gly-Leu]$^+$ and ninhydrin. *J. Mol. Liq.* **2019**, *274*, 639-645, DOI: 10.1016/j.molliq.2018.11.035.

[2] Siddiqui, F. A.; Sher, N.; Shafi, N.; Shamshad, H.; Zubair, A., Kinetic and thermodynamic

spectrophotometric technique to estimate gabapentin in pharmaceutical formulations using ninhydrin. *J. Anal. Sci. Technol*. **2013**, *4.1*, 1-8, DOI: 10.1186/2093-3371-4-17.

[3] Akram, M.; Rafiquee, M. Z.; Khan, Z., Micellar and salt effects on the rate of the condensation between ninhydrin and $[Cr(his)(H_2O)_3]^{2+}$, *Colloids Surf. A*. **2001**, *178*, 167-176, DOI: 10.1016/S0927-7757(00)00695-6.

[4] Khan, A. B.; Bhattarai, A.; Jaffari, Z. H.; Saha, B.; Kumar, D., Role of dimeric gemini surfactant system on kinetic study of alanine amino acid with ninhydrin reaction. *Colloid and Polymer Sci*. **2021**, *299.8*, 1285-1294, DOI: 10.1007/s00396-021-04847-0.

[5] Kumar, D.; Rub, M. A., Interaction of Metal Ion-Coordinated Dipeptide Complex and Ninhydrin in the Alkanediyl-α, ω-bis-Type Gemini Surfactant System. *J. Surf. and Deterg*. **2019**, *22.6*, 1299-1308, DOI: 10.1002/jsde.12340.

[6] Kumar, D.; Rub, M. A.; Asiri, A. M., Synthesis and characterization of geminis and implications of their micellar solution on ninhydrin and metal amino acid complex. *R. Soc. Open Sci*. **2020**, *7.7*, 200775, DOI: 10.1098/rsos.200775.

[7] Fry, B.; Carter, J. F.; Yamada, K.; Yoshida, N.; Juchelka, D., Position-specific 13C/12C analysis of amino acid carboxyl groups–automated flow-injection analysis based on reaction with ninhydrin. *R. C. MS*. **2018**, *32.12*, 992-1000, DOI: 10.1002/rcm.8126.

[8] Omar, K. A.; Sadeghi, R., Novel ninhydrin-based deep eutectic solvents for amino acid detection. *J. Mol. Liq.* **2020**, *303*, 112644, DOI: 10.1016/j.molliq.2020.112644.

[9] Friedman, M., Applications of the ninhydrin reaction for analysis of amino acids, peptides, and proteins to agricultural and biomedical sciences, *J. Agric. Food Chem.* **2004**, *52*, 385-404, DOI: 10.1021/jf030490p.

[10] Shi, J.; Chen, C.; Wang, D.; Wang, Z.; Liu, Y., The antimicrobial peptide LI14 combats multidrug-resistant bacterial infections. *Commun. Biol.* **2022**, *5*(1), 1-14, DOI: 10.1038/s42003-022-03899-4.

[11] Gough, E. K., The impact of mass drug administration of antibiotics on the gut microbiota of target populations. *Infect. Dis. Poverty* **2022**, *11*(1), 1-20, DOI: 10.1186/s40249-022-00999-5.

[12] Brochado, A. R.; Telzerow, A.; Bobonis, J.; Banzhaf, M.; Mateus, A.; Selkrig, J.; Typas, A., Species-specific activity of antibacterial drug combinations. *Nature* **2018**, *559*(7713), 259-263, DOI: 10.1038/s41586-018-0278-9.

[13] Delcour, A. H., Outer membrane permeability and antibiotic resistance. *(BBA)-Proteins and Proteomics* **2009**, *1794*(5), 808-816, DOI: 10.1016/j.bbapap.2008.11.005.

[14] Pshenay-Severin, E.; Bae, H.; Reichwald, K.; Matz, G.; Bierlich, J.; Kobelke, J.; Popp, J., Multimodal nonlinear endomicroscopic imaging probe using a double-core double-clad fiber and focus-combining micro-optical concept. *Light: Sci. Appl.* **2021**, *10*(1), 1-11, DOI: 10.1038/s41377-021-00648-w.

[15] Burley, J. C.; Van De Streek, J.; Stephens, P. W., CSD Entry: AMPCIH01. Cambridge Structural Database: Access Structures. *Camb. Crystallo. Data Centre.* **2006**, DOI: 10.5517/ccb0nkj.

[16] Burley, J. C.; van de Streek, J.; Stephens, P. W., Ampicillin trihydrate from synchrotron powder diffraction data. *Acta Crystallogr. E.* **2006**, *62*(2), 797-799, DOI: 10.1107/S1600536806001371.

[17] Akova, M., Sulbactam-containing β-lactamase inhibitor combinations. *Clin. Microbiol. Infect.* **2008**, *14*, 185-188, DOI: 10.1111/j.1469-0691.2007.01847.

[18] Suleyman, G.; Zervos, M. J., Safety and efficacy of commonly used antimicrobial agents in the treatment of enterococcal infections: a review. *Expert Opin. Drug Saf.* **2016**, *15*(2), 153-67, DOI: 10.1517/14740338.2016.1127349.

[19] Abdel-Khalek, A. A.; Adawi, A. M.; Abdel-Hafeez, M. M., Two-step one-electron transfer reaction of chromium(III) complex containing levodopa and uridine with N-bromosuccinimide. *J. Coord. Chem.* **2012**, *65*(8), 1324-1338, DOI: 10.1080/00958972.2012.671939.

[20] Jézéquel, T.; Joubert, V.; Giraudeau, P.; Remaud, G. S.; Akoka, S., The new face of isotopic NMR at natural abundance. *Magn. Reson. Chem.* **2017**, *55.2*, 77-90, DOI: 10.1002/mrc.4548.

[21] Bayle, K.; Grand, M.; Chaintreau, A.; Robins, R. J.; Fieber, W.; Sommer, H.; Remaud, G. S., Internal referencing for 13C position-specific isotope analysis

measured by NMR spectrometry. *Anal. Chem.* **2015**, *87.15*, 7550-7554, DOI: 10.1021/acs.analchem.5b02094.

[22] Joubert, V.; Silvestre, V.; Ladroue, V.; Besacier, F.; Blondel, P.; Akoka, S.; Remaud, G. S., Forensic application of position-specific isotopic analysis of trinitrotoluene (TNT) by NMR to determine 13C and 15N intramolecular isotopic profiles. *Talanta* **2020**, *213*, 120819, DOI: 10.1016/j.talanta.2020.120819.

[23] Khan, R. H., Tellurium mediated reduction of aromatic nitro groups. *J. Chem. Res.* **2000**, *6*, 290-291, DOI: 10.3184/030823400103167336.

[24] Ansari, T. M.; Raza, A.; Rehman, A. U., Spectrophotometric determination of tranexamic acid in pharmaceutical bulk and dosage forms, *Anal. Sci.* **2005**, *21*(9), 1133-1135, DOI: 10.2116/analsci.21.1133.

[25] Remaud, G.; Guillou, C.; Vallet, C.; Martin, G. J., A coupled NMR and MS isotopic method for the authentication of natural vinegars. *Fresenius J. Anal. Chem.* **1992**, *342*(4), 457-461, DOI: 10.1007/BF00322207.

[26] Khlebnikov, V.; Wijnen, J.; van der Kemp, W. J.; Klomp, D. W., 31P MRSI studies in patients with cancer, *Annu. Rep. NMR Spectrosc.* **2016**, *87*, 319-368, DOI: 10.1016/bs.arnmr.2015.08.004.

[27] Arayne, M. S.; Sultana, N.; Siddiqui, F. A.; Mirza, A. Z.; Zuberi, M. H., Spectrophotometric techniques to determine tranexamic acid: Kinetic studies using ninhydrin and direct measuring using ferric chloride. *J. Mol. Struct.* **2008**, *891*(1-3), 475-480, DOI: 10.1016/j.molstruc.2008.04.026.

[28] Pandey, E.; Upadhyay, S. K., Hydrotropic Enhancement of Rate of Ninhydrin-α-Amino Acid Reaction: A Kinetic Study. *J. Dispers. Sci. Technol.* **2006**, *27*(2), 213-218, DOI: 10.1080/01932690500266993.

[29] Bano, M.; Khan, I. A., kinetics and mechanism of the ninhydrin reaction with DL-methionine in the absence and presence of organic solvents, *Ind. J. Chem.* **2003**, *42B*, 1132-2236, DOI: 10.1021/acs.iecr.1c03184.